

# PROPOSAL TO PAC20

## Measurement of $G_{Ep}/G_{Mp}$ to $Q^2=9 \text{ GeV}^2$ via recoil polarization

**C.F. Perdrisat (co-spokesperson), T. Averett, O. Gayou<sup>†</sup>  
and L.P. Pentchev<sup>††</sup>**

*College of William and Mary*

**V. Punjabi (co-spokesperson), M. Khandaker and C. Salgado**

*Norfolk State University*

**M.K. Jones (co-spokesperson), R. Carlini, E. Chudakov, R. Ent,  
K. Garrow, J. Gomez, H. Fenker, N. Liyanage, A. Lung, D. Mack,  
D. Meekins, G. Smith, W. Vulcan, B. Wojtsekhowski**

*Jefferson Lab*

**E. Brash (co-spokesperson), G. Huber, A. Kozlov, G. Lolos,  
Z. Papandreou**

*University of Regina, Canada*

**J. Arrington, F. Dohrmann, K. Hafidi, R.J. Holt, H.E. Jackson,  
D.H. Potterveld, P.E. Reimer and K. Wijesooriya**

*Argonne National Laboratory*

**M. Epstein and D. Margaziotis**  
*California State University at Los Angeles*

**L. Todor**

*Carnegie Mellon University*

**E. Tomasi-Gustafsson**

*DAPNIA, Saclay, France*

**C. Howell, S. Churchwell**

*Duke University/TUNL*

**B. Milbrath**

*Eastern Kentucky University*

**W. Boeglin, P. Markowitz, B. Raue, J. Reinhold**

*Florida International University and Jefferson Lab*

**K. Baker, A. Gasparian, C. Keppel**

*Hampton University*

**A. Nathan**  
*University of Illinois*

**L. Bimbot**  
*Institut de Physique Nucléaire, Orsay, France*

**N. Merenkov**  
*Institute of Physics and Technology, Kharkov, Ukraine*

**C. C. Chang, J. Kelly**  
*University of Maryland*

**V.P. Kubarovsky, Yu.M. Goncharenko, A.P. Meschanin,**  
**L.F. Soloviev and A.N. Vasiliev**  
*Institute for High Energy Physics, Protvino, Russia*

**E. Cisbani, S. Frullani, F. Garibaldi, F. Cusanno**  
*INFN-ISS, Italy*

**M. Iodice**  
*INFN-Roma3, Italy*

**G.M. Urcioli**  
*INFN-Roma1, Italy*

**R. de Leo**  
*INFN-Bari, Italy*

**K. Fissum**  
*University of Lund, Sweden*

**N. Piskunov, D. Kirillov, I. Sitnik, and**  
**Yu. Zanesvky, S. Chernenko, L. Smykov and D. Fateev**  
*Laboratory for High Energy, JINR, Dubna, Russia*

**W. Bertozzi, S. Gilad, D. Higinbotham, S. Sirca, R. Suleiman,**  
**Z. Zhou**  
*Massachusetts Institute of Technology*

**M. Rekalo**  
*Middle East Technical University, Turkey*

**J. Calarco and O. Filoti**  
*University of New Hampshire*

**A. Afanasev, I. Akushevich and B. Vlahovic**  
*North Carolina Central University*

**R. Segel**

*Northwestern University*

**A. Radyushkin, P. Ulmer**

*Old Dominion University*

**F. Benmokhtar, S. Dieterich, R. Gilman, C. Glashausser, X. Jiang,**

**G. Kumbartzki, R. Ransome and S. Strauch**

*Rutgers University*

**H. Voskanian, K. Egiyan, A. Ketikyan, E. Hovhannisyan,**

**S. Mayilyan, A. Shahinyan**

*Yerevan Physics Institute, Armenia*

\* The name of collaborators assuming responsibility for development of a part of the instrumentation are underlined.

<sup>†</sup> also Université Blaise Pascal, Clermont-Ferrand, France

<sup>††</sup> also INRNE, Sofia, Bulgaria

## Abstract

In experiment 93-027 and 99-007, we measured with high precision the ratio of the electromagnetic elastic form factors of the proton,  $G_{Ep}/G_{Mp}$ , up to four-momentum transfer  $Q^2$  of 3.5 GeV<sup>2</sup> and 5.6 GeV<sup>2</sup>, respectively, with the recoil polarization technique. The data from these two JLab experiments have shown an unexpected and significantly different  $Q^2$ -dependence for the electric and magnetic form factors, starting at  $Q^2=1$  GeV<sup>2</sup>, up to the maximum value of 5.6 GeV<sup>2</sup>, revealing a definite difference in spatial distribution of charge and magnetization at short distances. These data also clearly demonstrate that we have not yet reached the perturbative QCD limit, which would be signaled by the ratio  $Q^2 F_{2p}/F_{1p}$  becoming constant. The new results have created great interest, both theoretically and experimentally, emphasizing the importance of continuing the  $G_{Ep}/G_{Mp}$  ratio measurements to higher  $Q^2$ .

Here, we propose to measure the ratio  $G_{Ep}/G_{Mp}$  in Hall C with the recoil polarization technique, to  $Q^2=9$  GeV<sup>2</sup> in elastic electron scattering from hydrogen with a 6 GeV incident electron beam energy. The proton will be detected in the high momentum spectrometer and the electron in a large solid angle lead glass calorimeter, as was done recently in experiment 99-007.

The proposed data, together with the  $G_{Mp}$  extracted from cross section data, will determine both  $F_{1p}$  and  $F_{2p}$ , the Dirac and Pauli form factors, separately. At large  $Q^2$ ,  $F_{1p}$  was obtained from cross section measurements and assuming  $\mu G_{Ep} = G_{Mp}$ . Extrapolating the new results from Jlab would result in a 14% change in the  $F_{1p}$  values above  $Q^2$  of 10 GeV<sup>2</sup>.

This experiment will extend the knowledge of  $F_{2p}$ , which is equally sensitive to  $G_{Ep}$  and  $G_{Mp}$ , and it will also determine  $F_{1p}$  accurately in the same  $Q^2$  region. This  $Q^2$  region is thought to be the one of transition between soft and hard scattering, and is the most challenging theoretically. The data from this experiment will give insight into this intermediate region and as such, provide a testing ground for future theoretical developments.

**This experiment requires 6 GeV incident electron energy, and thus can be done before the anticipated energy upgrade of the CEBAF accelerator. After the CEBAF upgrade the ratio  $G_{Ep}/G_{Mp}$  can be measured to  $Q^2 = 12$  GeV<sup>2</sup> with the existing HMS.**

# 1 Introduction

In 1998, experiment 93-027 measured the ratio  $G_{Ep}/G_{Mp}$  in Hall A, with high precision. These data are now published[1]. At the end of 2000, these measurements were continued with experiment 99-007, which extended the range of  $Q^2$ -values to 5.6  $\text{GeV}^2$ . The results from experiment 99-007 are still PRELIMINARY and they are shown together with those of experiment 93-027 and world data in Fig. 1.

The most important feature of the new JLab data is the sharp decline of the ratio  $G_{Ep}/G_{Mp}$  as  $Q^2$  increases, definitively showing that  $G_{Ep}$  falls faster than  $G_{Mp}$ . This is the first experimental evidence that the  $Q^2$ -dependence of  $G_{Ep}$  and  $G_{Mp}$  is definitely different starting at 1  $\text{GeV}^2$ . These new data for  $G_{Ep}$  have created much excitement in the Nuclear Physics community, and an intriguing question is whether  $G_{Ep}/G_{Mp}$  will continue to decrease and become negative, or ultimately will become constant with increasing  $Q^2$ .

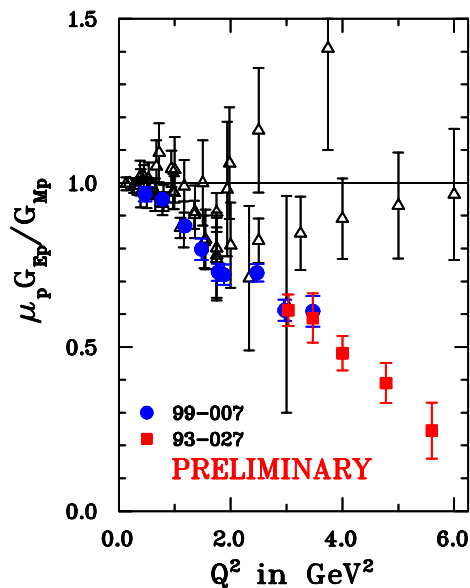


Figure 1: The ratio  $\mu_p G_{Ep}/G_{Mp}$  as determined in experiments 93-027 and 99-007 (filled symbols), compared to world data (open symbols) [2, 3, 4, 5, 6, 7]; the uncertainties shown for both experiments are statistical only; the systematic uncertainties are of similar size.

The ratio  $G_{Ep}/G_{Mp}$  from Jlab data can be used to obtain  $G_{Ep}/G_D$  values using the parametrization of  $G_{Mp}/G_D$  of Bosted [8]; where  $G_D = 0.71^2(0.71 + Q^2)^{-2}$  is the dipole form factor.  $G_{Ep}/G_D$  and  $G_{mp}/G_D$  are shown in Figs. 2

and 3 to highlight the drastically different  $Q^2$ -behavior of  $G_{Ep}$  and  $G_{Mp}$ . The Bosted parametrization of  $G_{Mp}/G_D$  is affected by the JLab ratio data at the 1% level in the range 1.75 to 8.85  $\text{GeV}^2$  [9].

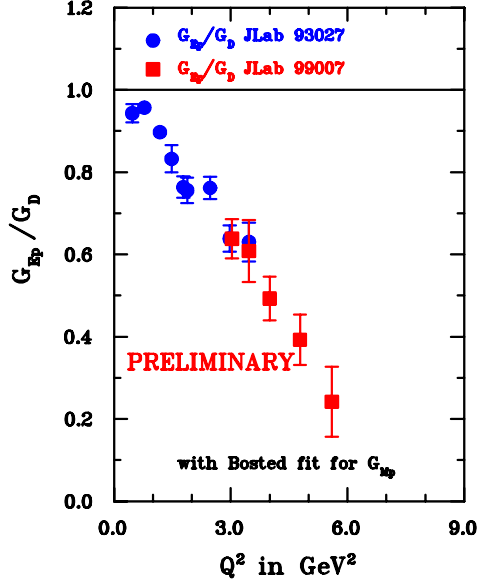


Figure 2: The JLab data as  $G_{Ep}/G_D$ : dots 93-027, squares 99-007; the new data deviates strongly from the dipole form factor value of 1.

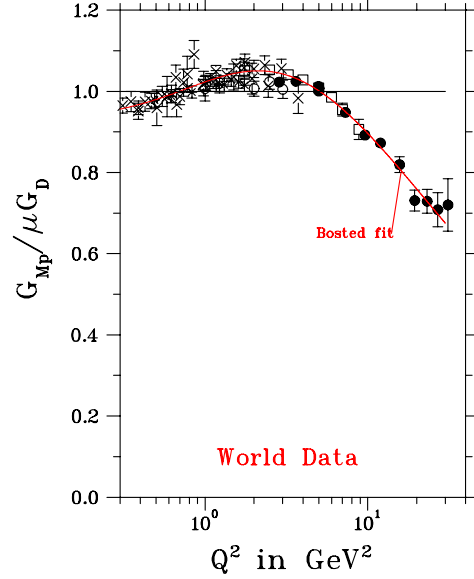


Figure 3: World data for  $G_{Mp}/G_D$ , showing that the dipole form factor describes the experimental magnetic form factor within 10% below 9  $\text{GeV}^2$ . The curve is the Bosted [8] fit.

In a proposal submitted to PAC18 in July, 2000 (proposal 00-111)[10], we showed that it is now possible to extend the measurement of the  $G_{Ep}/G_{Mp}$  ratio to yet higher  $Q^2$  values at JLab in Hall C. This proposal was deferred; reasons given included:

- 1) a request for information regarding the support and additional equipment required from the laboratory (see part 6), and
- 2) a suggestion that the new apparatus (the focal plane polarimeter) be designed with the aim of incorporating the capability to run ultimately at the highest  $Q^2$  that would be possible with a future accelerator upgrade to 12  $\text{GeV}$  (see page 18).

We will address these concerns in this proposal.

The proposed experiment requires a new focal plane polarimeter (FPP) in Hall C, and a large area lead-glass calorimeter to detect the electron:

- 1) we have a design and cost estimate for the FPP in part 6, and
- 2) for the calorimeter, 700 lead-glass blocks (from Hall A RCS experiment) are

already at JLab and an additional 1000 lead-glass blocks (from Fermilab and belonging to the Protvino group) will be at JLab shortly; also, we have negotiated with Fermilab to borrow the ADCs and TDCs and auxiliary equipment (fastbus crates, low voltage power supplies and so on) required for the calorimeter for the duration of the preparation and run of this experiment. This proposal needs to be approved at this time, because the construction, installation and testing of the new equipment will take about three years.

With the addition of a FPP in the HMS focal plane and a large area lead-glass calorimeter on the floor, to the standard equipment of Hall C [11], the recoil polarization technique can be used to measure the  $G_{Ep}/G_{Mp}$  ratio up to  $Q^2$  of 9 GeV<sup>2</sup>.

The results of experiment 99-007 also determined the analyzing power for CH<sub>2</sub> up to proton momentum of 3.8 GeV/c. From these data, we are able to extrapolate the analyzing power up to proton momentum of 5.7 GeV/c, corresponding to  $Q^2 = 9$  GeV<sup>2</sup>. The absolute uncertainties on these new data will be similar to those of experiment 99-007. The beam energy required is 6 GeV.

With regards to point 2 of PAC18's concerns: with a 12 GeV upgrade at JLab, it would become possible to extend the  $Q^2$  range for  $G_{Ep}$  to approximately 12 GeV<sup>2</sup> with the HMS equipped with the new FPP and with the new calorimeter. Also, several other experiments would benefit from the new FPP and the calorimeter in Hall C. Like the present proposal, they are direct extensions of existing Hall A polarization measurements, that will take advantage of the higher central momentum and larger acceptance of the Hall C spectrometer. Being currently considered are the deuteron photo-disintegration measurements of induced and transferred polarization in  $^2H(\vec{\gamma}, \vec{p})n$ , (Hall A experiments 89-019[12]),  $\pi^0$  photo-production from the proton,  $^1H(\vec{\gamma}, \vec{p})\pi^0$  (Hall A experiment 94-012[13]), and real Compton scattering to larger  $t$  values (Hall A experiment 99-114[14]).

Based on the pp database it appears likely that the analyzing power would go through zero near proton momentum of 10 GeV/c, corresponding to  $Q^2 = 17$  GeV<sup>2</sup>, a natural hard limit to the extension of the polarization measurement of the  $G_{Ep}/G_{Mp}$  ratio. A realistic limit may be 14 GeV<sup>2</sup>, requiring an 8.5 GeV/c spectrometer with no more than 20° bending angle and at least 10 msr solid angle. So 12 GeV will make it possible to measure 2 more  $Q^2$  values, 10.5 and 12.4 GeV<sup>2</sup> with the HMS, with its capability to detect 7.5 GeV/c protons, and with the new FPP we are proposing to build. Neither the planned SHMS in Hall C nor MAD in Hall A will be usable for this continuation: the SHMS acceptance is at least 5 times too small, and the maximum accepted momentum in MAD is only 6 GeV/C.

**There is no other accelerator and detector facility in the world where the proposed measurements could be made.**

## 2 Physics Interest

The characterization of the structure of the nucleon is the defining problem of hadronic physics, as the hydrogen atom is to atomic physics. Elastic nucleon form factors are key ingredients of this characterization. Ideally, all four elastic nucleon form factors should be measured to the highest possible  $Q^2$ . The independent determination of  $G_{Mp}$  and  $G_{Ep}$  from the unpolarized ep cross section data has been done up to  $Q^2 = 8.8 \text{ GeV}^2$  [2]. The extraction of  $G_{Mp}$  from a single cross section measurement, to higher  $Q^2$  assumes  $\mu_p G_{Ep} = G_{Mp}$  [15]; these data are shown in Fig. 3. New measurements of  $G_{Mn}$  in Hall B [16] are currently being analyzed; they will bring the knowledge of this form factor to comparable levels of accuracy up to  $Q^2=4.8 \text{ GeV}^2$ . For the neutron electric form factor, two new JLab experiments 93-026[17] and 93-038[18] will extend the  $Q^2$  range to  $1.5 \text{ GeV}^2$ , with an accuracy comparable to the 3 other form factors. The experiment we are proposing here extends the range over which  $G_{Ep}$  will be accurately measured to a  $Q^2$  of  $9 \text{ GeV}^2$ .

In exclusive electron scattering at high  $Q^2$ , the dominant degrees of freedom of the nucleon are the three valence quarks. This is the regime where perturbative QCD theory can be applied [19]. At  $Q^2 < 1 \text{ GeV}^2$ , the Vector Meson Dominance (VMD) model [20, 21, 22] has been successful in describing the nucleon form factors and hadronic interactions. Predicting nucleon form factors in the intermediate  $1 < Q^2 < 20 \text{ GeV}^2$  region, where soft scattering processes are still dominant compared to hard scattering, is very difficult. There is also some controversy over where this transition regime starts. The evidence provided by JLab experiments 93-027 and 99-007, that the  $Q^2$  dependence of  $G_{Ep}$  and  $G_{Mp}$  is different, suggests that their soft contributions are different. This fact can be used as a tool to understand the role of the soft parts of the proton without having to reach asymptotically high  $Q^2$ .

Currently, many QCD models are used to calculate the elastic nucleon form factors, including the following: the relativistic constituent quark model (RCQM)[23, 24, 25], the di-quark model [26], QCD sum rules [27], and the cloudy bag model [28]. There is a soliton model calculation [29] which uses the skyrmion as an extended object; this model successfully describes our data. A sample from the preceding theoretical predictions is shown, together with the JLab-data, in Fig. 4. Several new calculations with the RCQM have been motivated by the results of 93-027 [30, 31, 32]; the data are reproduced when relativistic effects left out of previous calculations are included; in [30] it is pointed out that within the framework of the RCQM, the data appear to be directly sensitive to the structure of the proton wave function. It should be obvious that any calculation of nucleon isobar properties, like transition amplitudes, must first describe the nucleon form factor data.

The helicity conserving Dirac form factor,  $F_{1p}$ , describes the spread-out charge and Dirac magnetic moment, and the helicity non-conserving Pauli form factor,  $F_{2p}$ , the spread-out Pauli magnetic moment; these two form factors are



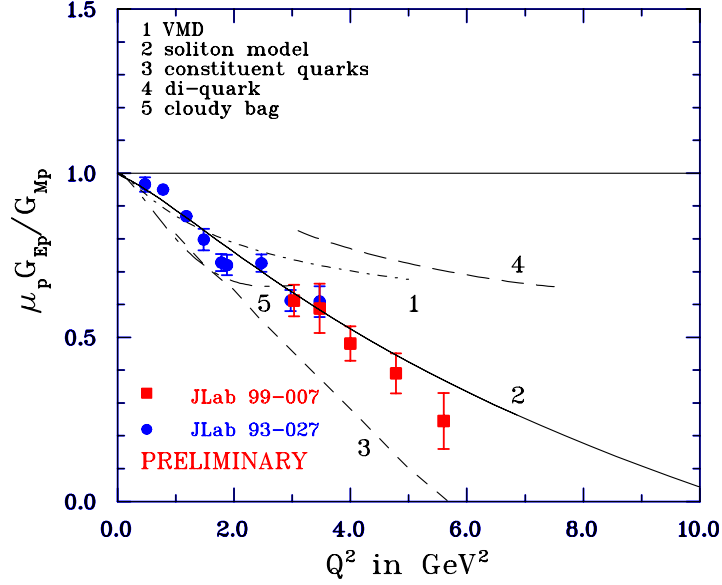


Figure 4: Comparison of JLab data with several theoretical predictions.

the key ingredients of the hadronic current. The Sachs form factors,  $G_{Ep}$  and  $G_{Mp}$ , which are easier to extract directly from the data, are related to  $F_{1p}$  and  $F_{2p}$ , by the following equations:

$$F_{1p} = \frac{G_{Ep} + \tau G_{Mp}}{1 + \tau} \text{ and } F_{2p} = \frac{G_{Mp} - G_{Ep}}{\kappa_p(1 + \tau)} \quad (1)$$

where  $\tau = Q^2/4m^2$  and  $\kappa_p$  is the proton anomalous magnetic moment.

In the pQCD approach  $F_{1p}$  has a  $Q^{-4}$  dependence and  $F_{2p}$  has a  $Q^{-6}$  dependence; hence pQCD predicts that  $Q^2 F_{2p}/F_{1p}$  should become constant at high  $Q^2$ , as suggested first by Brodsky and Farrar [19] and later discussed in detail by Brodsky and Lepage[33].

As seen in Eq. 1,  $F_{1p}$  is dominated by  $G_{Mp}$  at high  $Q^2$  because of the multiplicative factor  $\tau$ . Although the approximate flattening of  $Q^4 F_1$  as seen in Fig. 5 at  $Q^2 > 10 \text{ GeV}^2$  is often identified as pQCD scaling, it can also be interpreted as the interplay between soft and hard scattering. Fig. 5 also shows that JLab results require new analysis of the Sill [15] data, as their extraction of  $F_{1p}$  from cross section data was based on assumption  $\mu G_{Ep} = G_{Mp}$ . Extrapolating the new results from Jlab produces 14% change in the  $F_{1p}$  values of ref. [15] near  $Q^2$  of  $10 \text{ GeV}^2$ .

In contrast to  $F_{1p}$ ,  $F_{2p}$  contains equal contributions from  $G_{Ep}$  and  $G_{Mp}$  at

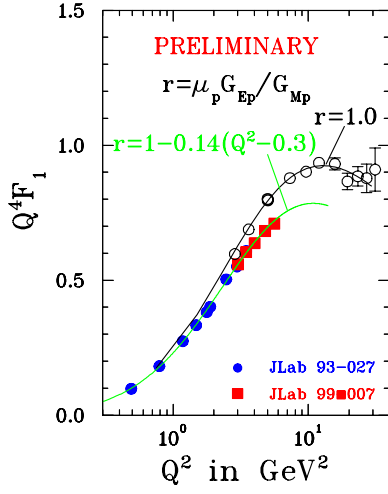


Figure 5: Data of Sill et al.[15], (open symbols) compared to JLab data (filled symbols). The approximate flattening of  $Q^4 F_1$  at  $Q^2 \sim 10 \text{ GeV}^2$  is often interpreted as pQCD scaling.

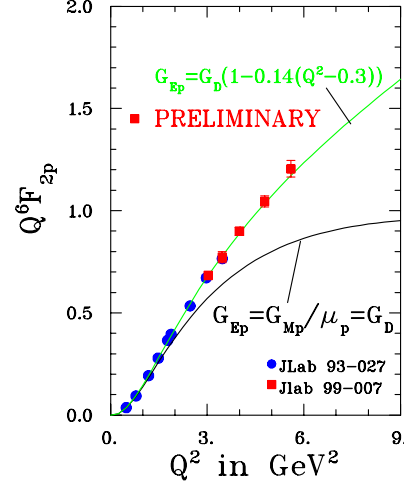


Figure 6: The points are calculated using  $G_{Ep}/G_{Mp}$  of 93-027 and 99-007, and  $G_{Mp}$  from the Bosted fit to world data.

all  $Q^2$ s. So  $F_{2p}$  cannot be determined accurately without  $G_{Ep}$  data. In Fig. 6, we show the values of  $Q^6 F_{2p}$  obtained by combining the new JLab  $G_{Ep}/G_{Mp}$  data with  $G_{Mp}$  values from the Bosted [8] fit to the world data. Within the range of  $Q^2$  mapped so far by the JLab data, no constant values is reached.

Of course, a critical question is: what will be the  $Q^2$  dependence of  $F_{2p}$  in the  $Q^2$  range of this proposal, in particular will  $Q^6 F_{2p}$  reach a constant value? The answer to this question can only be supplied by data from the proposed experiment.

In Fig. 7, we show  $Q^2 F_{2p}/F_{1p}$  extracted directly from the JLab experiments 93-027 and 99-007, and the data of ref. [2] As:

$$\frac{F_2}{F_1} = \frac{1 - G_E/G_M}{\kappa_p(\tau + G_E/G_M)}, \quad (2)$$

there is no need of  $G_{Mp}$ -data to obtain this ratio; we measure  $G_{Ep}/G_{Mp}$ . What appeared to be an early flattening of the  $Q^2 F_{2p}/F_{1p}$  ratio to a constant value[2], is definitely not confirmed by the JLab data.

In Fig. 8 the JLab data plotted as  $Q F_{1p}/F_{2p}$  show a remarkable flattening of the ratio starting at 1-2  $\text{GeV}^2$ . Inspired by the results of JLab experiment 93-027, Ralston [34] revisited the calculation of the single-quark spin flip amplitude responsible for the Pauli form factor in the framework of QCD. According to Ralston [34] if quarks in the proton carry orbital angular momentum (of a

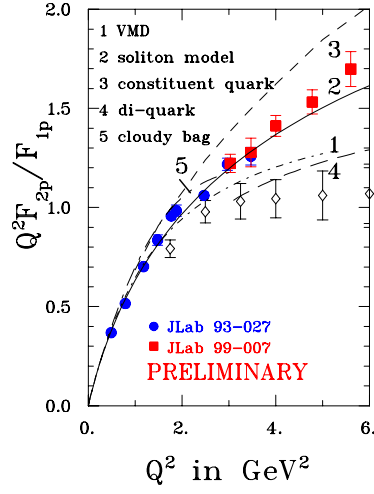


Figure 7: The ratio  $F_2/F_1$  times  $Q^2$  extracted directly from the data of experiments 93-027 and 99-007; open symbols for the data of [2]

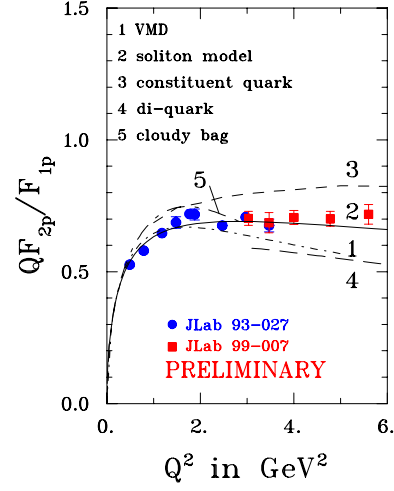


Figure 8: The ratio  $F_2/F_1$  multiplied by  $\sqrt{Q^2}$ , discussed in relation to the calculation of ref[34].

particular gauge-invariant kind), then  $F_{1p}/F_{2p}$  should behave like  $\frac{1}{\sqrt{(Q^2)}}$ , rather than the well known pQCD prediction of  $\frac{1}{Q^2}$  (ref. [19]), and the  $\frac{1}{\sqrt{(Q^2)}}$  behavior should set in at  $Q^2 \sim 1-2 \text{ GeV}^2$ , as seen in Fig. 8.

Recent theoretical developments also indicate that measurements of the separated elastic form factors of the nucleon to high  $Q^2$  may shed light on the problem of nucleon spin. This connection between elastic form factors and spin has been demonstrated within the formalism of Generalized Parton Distributions (GPD). The first moment of the GPD taken in the forward limit yields, according to the Angular Momentum Sum Rule [35], a contribution to the nucleon spin from the quarks and gluons, including both the quark spin and orbital angular momentum. The  $t$ -dependence of the GPDs has been modeled using a factor corresponding to the relativistic Gaussian dependence of both Dirac [36] and Pauli [37] form factors of the proton. Extrapolation of these GPDs to  $t=0$  leads to the functions entering into the Angular Momentum Sum Rule, and an estimate of the contribution of the valence quarks to the proton spin can then be obtained. This approach was used recently by Afanasev [38] who, using the  $G_{Ep}/G_{Mp}$  data of experiment 93-027 in the framework of GPD, concluded that valence quarks contribute about 50% to the nucleon spin. When combined with inclusive deep inelastic scattering data from SMC [39], this result implies that about 25% of the proton spin comes from the orbital angular momentum of the valence quarks.

There are also lattice QCD calculations predicting the contribution to the proton spin coming from angular momentum of the valence quarks. For example, Mathur et al. [40] calculate the quark orbital angular momentum of the proton from the quark energy-momentum tensor form factors on the lattice. They calculate the total contribution from the quarks to be 60%, and hence 35% of the proton spin originates from the orbital angular momentum. These calculations are performed in a rigorous and gauge invariant formalism, and the general agreement with the GPD analysis of Afanasev is encouraging. An extension of the measurements of the  $G_{Ep}/G_{Mp}$  ratio to higher momentum transfers will help constrain the  $x$ -dependence of the GPD and represent an important step towards a characterization of the quark spin and orbital angular momentum contributions to the proton spin.

We also point out that there is a major effort to use lattice QCD to understand the structure and interaction of hadrons, spear-headed by Isgur and Negele [41]. The nucleon form factors are an important first phase of the program.

### 3 The Recoil Polarization Method

In 1974 Akhiezer and Rekalov [42] discussed the interest of measuring an interference term of the form  $G_E G_M$  by measuring the transverse component of the recoiling proton polarization in  $\bar{e}p \rightarrow e\bar{p}$  at large  $Q^2$ , to obtain  $G_E$  in the presence of a dominating  $G_M$ . This method was later discussed in more detail by Arnold, Carlson, and Gross [43]. Indeed, the recoil polarization method has been used successfully to measure the ratio  $G_{Ep}/G_{Mp}$  up to  $Q^2 = 5.6 \text{ GeV}^2$  in JLab experiments 93-027 and 99-007. Here, we are proposing to use this technique to measure the  $G_{Ep}/G_{Mp}$ -ratio to  $Q^2 = 9.0 \text{ GeV}^2$ .

The three components of the polarization for the outgoing proton are expressed in the  $(\hat{n}, \hat{l}, \hat{t})$  helicity basis, where  $\hat{l}$  is the unit vector in the direction of the proton momentum,  $\hat{n}$  is perpendicular to the reaction plane, and  $\hat{t} = \hat{n} \times \hat{l}$  is the transverse unit vector. For elastic ep scattering with a longitudinally polarized electron beam, the only non-zero polarization transfer observables are the longitudinal and transverse polarizations,  $P_l$  and  $P_t$ . Above  $Q^2=1 \text{ GeV}^2$  the electric part of the elastic cross section is dropping rapidly ( $\sim 0.5\%$  of  $\sigma_{ep}$  at  $Q^2 = 5.6 \text{ GeV}^2$ ), making the Rosenbluth separation exceedingly difficult. The advantages are that a) recoil polarization entails lower systematic uncertainties since no change in beam energy or detector arm angle is required, and b) the transverse polarization component is proportional to the interference term  $G_{Ep}G_{Mp}$ , and hence not so small. For single photon exchange, the transferred polarization can be written in terms of the Sachs form factors as [42, 43]:

$$P_n = 0 \quad (3)$$

$$P_t = \left( \frac{E_e + E'_e}{M} \right) \frac{\sqrt{\tau(1+\tau)} G_{Mp}^2(Q^2) \tan^2 \frac{\theta_e}{2}}{G_{Ep}^2(Q^2) + \frac{\tau}{\epsilon_\gamma} G_{Mp}^2(Q^2)} \quad (4)$$

$$P_t = \frac{2\sqrt{\tau(1+\tau)} G_{Ep} G_{Mp} \tan \frac{\theta_e}{2}}{G_{Ep}^2(Q^2) + \frac{\tau}{\epsilon_\gamma} G_{Mp}^2(Q^2)} \quad (5)$$

Here  $E_e$  and  $E_{e'}$  are the incident and scattered electron energies,  $\theta_e$  is the electron scattering angle, and  $M$  is the mass of the proton;  $\epsilon_\gamma = [1 + 2(1 + \tau) \tan^2 \frac{\theta_e}{2}]^{-1}$  is the longitudinal polarization of the virtual photon; the beam electrons are assumed to be fully polarized (helicity  $h=1$ ).

Combining Eq. 4 and 5 gives:

$$\frac{G_{Ep}}{G_{Mp}} = -\frac{P_t}{P_l} \frac{(E_e + E'_e)}{2M} \tan \frac{\theta_e}{2} \quad (6)$$

For each  $Q^2$ , a single measurement of the azimuthal angular distribution of the proton scattered in a secondary target gives both the longitudinal and transverse polarizations. Thus the ratio of electric to magnetic form factors of the proton is obtained directly from a simultaneous measurement of the two recoil polarization components. The kinematic factors in Eq. 6 are typically known to a precision far greater than the statistical precision of the recoil polarization components.

### 3.1 Focal Plane Polarimetry

The azimuthal distribution of the protons after scattering in the analyzer is given by:

$$\begin{aligned} N_p^\pm(\vartheta, \phi) &= N_p^\pm \left[ 1 + (\pm h A_y(\vartheta) P'_t + a_{inst} \sin \varphi + (\pm h A_y(\vartheta) P'_n + b_{inst}) \cos \varphi \right] \\ &= N_p^\pm \left[ 1 + (\pm a(\vartheta) + a_{inst}) \sin \varphi + (\pm b(\vartheta) + b_{inst}) \cos \varphi \right] \quad (7) \end{aligned}$$

where  $N_p^\pm$  is the number of protons incident on the analyzer,  $h$  is the helicity,  $A_y$  is the analyzing power,  $a_{inst}$  and  $b_{inst}$  are the instrumental asymmetries. It is important to note that the results of this experiment are based on the **difference** in azimuthal angular distributions of positive and negative electron helicities, and thus the instrumental asymmetries cancel.

### 3.2 Spin Precession

Typically, elastic  $ep$  events are identified by detecting both electron and proton in coincidence. In this experiment, the electron will be detected in a lead-glass

detector array (as was the case in E99-007), and the proton will be detected with the Hall C HMS. As a proton travels through the HMS, its spin precesses due to the interaction of the magnetic moment of the proton with the magnetic fields of the three quadrupoles and of the dipole. The relationship between the polarization components at the target and in the focal plane of the analyzer is given by the following spin transport matrix:

$$\begin{pmatrix} P'_n \\ P'_t \\ P'_l \end{pmatrix}_{\text{focal plane}} = \begin{pmatrix} S_{n'n} & S_{n't} & S_{n'l} \\ S_{t'n} & S_{t't} & S_{t'l} \\ S_{l'n} & S_{l't} & S_{l'l} \end{pmatrix} \begin{pmatrix} P_n \\ P_t \\ P_l \end{pmatrix}_{\text{target}}. \quad (8)$$

For the case of a single homogeneous dipole, the spin matrix would be given by:

$$\begin{pmatrix} S_{n'n} & S_{n't} & S_{n'l} \\ S_{t'n} & S_{t't} & S_{t'l} \\ S_{l'n} & S_{l't} & S_{l'l} \end{pmatrix} = \begin{pmatrix} \cos \chi & 0 & \sin \chi \\ 0 & 1 & 0 \\ -\sin \chi & 0 & \cos \chi \end{pmatrix} \quad (9)$$

where  $\chi$  is the spin precession angle given by  $\chi = \theta_B \gamma_p \kappa_p$ ;  $\theta_B$  is the bend angle in the dipole,  $\gamma_p = E_p/M$ , with  $E_p$  the proton energy, and  $\kappa_p$  is the anomalous part of the proton magnetic moment.

The Hall C HMS consists of three quadrupoles and one dipole with inclined edges and an index. These higher order magnetic fields cause further spin rotation that must be taken into account on an event by event basis. The result is a different spin matrix for each event that has nine non-zero matrix elements. The matrix elements are calculated using a modeling code such as COSY. Initial simulations done by A. Kozlov indicate that systematic uncertainties due to spin transport will be as small or smaller than achieved already in Hall A. In addition, we note that the optics matrix elements of the Hall C HMS are known very well, after many years of running experiments, and thus this contribution to the systematic uncertainty will be further minimized.

As  $P_n=0$  in elastic ep scattering, and we measure only  $P'_n$  and  $P'_t$  in the FPP, Eq. 8 reduces to:

$$P'_n = S_{n'l} P_l + S_{n't} P_t \quad \text{and} \quad P'_t = S_{t't} P_t + S_{t'l} P_l, \quad (10)$$

Then, with Fourier analysis and using Eq. 10, the Fourier amplitudes  $a(\vartheta)$  and  $b(\vartheta)$  as defined in Eq. 7 can be approximated as the sums over all events in the azimuthal distribution, as follows:

$$b(\vartheta) \approx \frac{2hA_y(\vartheta)}{N} \left[ P_t \cdot \sum_{i=1}^N S_{n'l}^{(i)} \cos^2 \varphi_i + P_l \cdot \sum_{i=1}^N S_{n't}^{(i)} \cos^2 \varphi_i \right] \quad (11)$$

$$a(\vartheta) \approx \frac{2hA_y(\vartheta)}{N} \left[ P_t \cdot \sum_{i=1}^N S_{t't}^{(i)} \sin^2 \varphi_i + P_l \cdot \sum_{i=1}^N S_{t'l}^{(i)} \sin^2 \varphi_i \right] \quad (12)$$

where  $i$  is the event index. One can solve Eq. 11 and 12 for the two unknowns  $hA_y(\vartheta)P_t$  and  $hA_y(\vartheta)P_\ell$ .

The ratio  $G_{Ep}/G_{Mp}$  can now be obtained directly from the ratio  $r(\vartheta) = \frac{hA_y(\vartheta)P_t}{hA_y(\vartheta)P_\ell}$ :

$$G_{Ep}/G_{Mp} = -r(\vartheta) \frac{(E_e + E_{e'})}{2M} \tan\left(\frac{\theta_e}{2}\right), \quad (13)$$

so that  $h$  and  $A_y$  cancel out.

The expression for  $P_t$  and  $P_\ell$  (Eqs. 4 and 5) can then be used to calculate these two components from the measured  $G_{Ep}/G_{Mp}$  leading to a calculation of the quantity  $hA_e(\vartheta)$ . The beam polarization will be measured independently with the Møller polarimeter in Hall C, thus providing a calibration of the polarimeter analyzing power for each of the proton energies of this proposal, which will be useful for future experiments using the FPP.

The radiation correction to the recoil polarization has been calculated by Afanasev et al [44]; the correction to the  $P_t/P_\ell$ -ratio remains smaller than 1% up to 5.6 GeV<sup>2</sup>; this calculation will be extended to the  $Q^2$  domain of this proposal.

## 4 Experimental considerations

### 4.1 Introduction

This experiment will use the High Momentum Spectrometer (HMS) in Hall C to detect the recoiling proton, and a new, large solid angle, calorimeter to detect the scattered electron. The focal plane in the HMS will be equipped with a polarimeter to measure the polarization of the recoil proton. The following subsections describe the modifications and additions to existing equipment in Hall C necessary to carry out this experiment.

#### 4.1.1 The High Momentum Spectrometer

The HMS bends charged particles in the vertical plane by 25°; it consists of 3 quadrupoles followed by one dipole. Its angular acceptance is 60x130 mr<sup>2</sup> in the horizontal and vertical direction, respectively, for a solid angle of 6 msr. The momentum bite ( $P_{max}-P_{min}$ )/ $P_0$  in HMS is 18% and the highest momentum accepted by the HMS is 7.5 GeV/c [45]. The angular resolution is 0.8 mr in both directions, the momentum resolution is  $< 10^{-3}$  and the y-resolution at the target is 1 mm; these resolutions are perfectly adequate for this experiment.

Favorable precession angles are desirable to obtain the ratio  $G_{Ep}/G_{Mp}$  with small uncertainty. In this experiment, we will extract  $P_t$  and  $P_\ell$  at the target from the measured quantities  $P'_t$  and  $P'_n$  at the analyzer; Eqs. 9 and 10 make it clear that  $\sin \chi=0$  must be avoided, otherwise  $P'_n=0$ . The precession angles corresponding to previously obtained data points and the 3 proposed data points

are shown in Fig. 9; all 3 angles are very favorable and actually the one corresponding to 9 GeV<sup>2</sup> is nearly the best possible (about 270°). The spectrometer

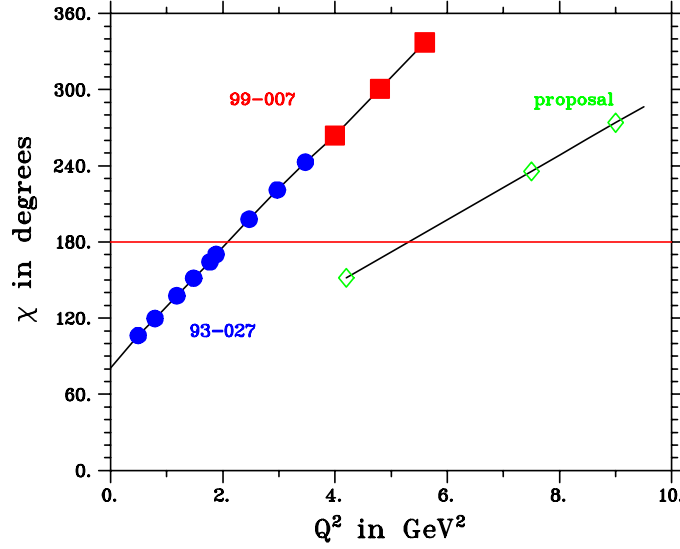


Figure 9: Diagram showing the precession angle  $\chi = \theta_B \gamma_p \kappa_p$  of all data points of experiments 93-027 and 99-007, as well as the proposed data points.

optics needs to be modeled precisely with a code like COSY, to calculate the spin transport coefficients with sufficient accuracy. Our recent studies of the optics of both HRS in Hall A has prepared us to undertake similar measurements in the HMS. In particular, the uncertainty on the coefficient  $S_{\nu\ell}$  in Eq. 10 is the main contribution to the systematic uncertainty on  $P_t$ , and therefore of  $G_{Ep}/G_{Mp}$ . Our studies have shown that  $S_{\nu\ell}$  depends upon the bending angle in the transverse plane ( $yz$ ),  $\phi$ . We will measure misalignment due to inaccuracy in placement of the magnetic elements of the HMS to control the corresponding uncertainty. At the highest  $Q^2$  of this proposal a systematic uncertainty (or error) on  $\phi$  of 0.3 mr produces an absolute uncertainty on  $\mu_p G_{Ep}/G_{Mp}$  of 0.04; this is to be compared with the goal of achieving an absolute statistical uncertainty on the point of 0.08. We note that the QQQD configuration of the HMS is advantageous because it is more symmetric for trajectories in the  $xz$  plane than the QQDQ configuration of the HRS.

#### 4.1.2 The Focal Plane Polarimeter

This experiment requires the installation of a new polarimeter in the focal plane area of the HMS. The new polarimeter will be located downstream of the scin-



tillators  $s1x$  and  $s1y$  as shown in Fig. 10; the analyzer will be divided into two blocks of  $\text{CH}_2$ , each 60 cm thick. The incoming proton trajectories will be reconstructed from the existing HMS focal plane drift chambers DC1 and DC2. Two new drift chambers with good angular resolution, of the design shown in Fig. 11, will follow each  $\text{CH}_2$  analyzer block to reconstruct the trajectory after the scattering in the analyzer, for a total of 4 chambers. There are at least two advantages to this configuration: first the chamber dimensions are smaller than when a single analyzer of equivalent thickness is used; and second, two polarimeters in series will provide better analyzing power and efficiency because events with nuclear scattering in both analyzer blocks can be analyzed separately.

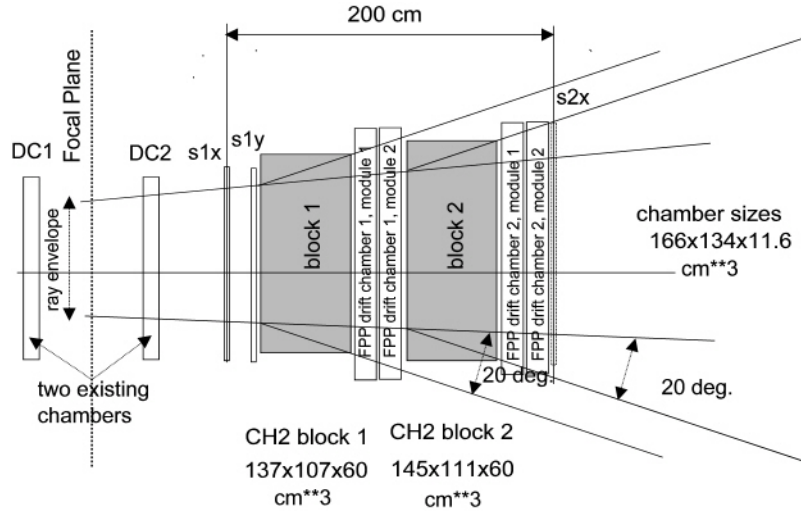


Figure 10: Side-view to scale, of the planned new polarimeter for the HMS (in the dispersive direction);  $s1x$  and  $s1y$  are the existing scintillator planes which will define the trigger.

The four new chambers required for this polarimeter will be identical; their sensitive area will be  $\sim 166 \times 134 \text{ cm}^2$ , as defined by the simulation and limitations of the space available in the HMS focal plane hut. The FPP design goals include approximately 100% track efficiency, 1 MHz singles rate with 1 % dead time and instrumental asymmetries of 0.005. This translates into  $100 \mu\text{m}$  position resolution per plane. Based on previous experience, we chose for the new polarimeter in Hall C, standard drift chambers with 2 cm distance between sense wires, and 2 cm between the interspersed field wires. The cathode wire planes have 0.3 cm spacing. The chamber dimensions are defined from the Hall C simulation package (simC). Our experience in Hall A makes us choose wire

orientations of  $\pm 45^\circ$  to the spectrometer x (dispersive) and y (transverse) coordinates. Each one of the 2 analyzer blocks will be followed by 6 wire planes (uvuvuv) to achieve the required angular resolution of 1 mr, with a spacing between the first and last plane of 15 cm. The resulting number of sense wires, amplifier/discriminator and shapers is 104 per plane, for a total of 1248 wires for the 12 planes. A detailed design plan has been prepared by the detector group of the Laboratory for High Energy at JINR/Dubna (leader Yuri Zanevsky).

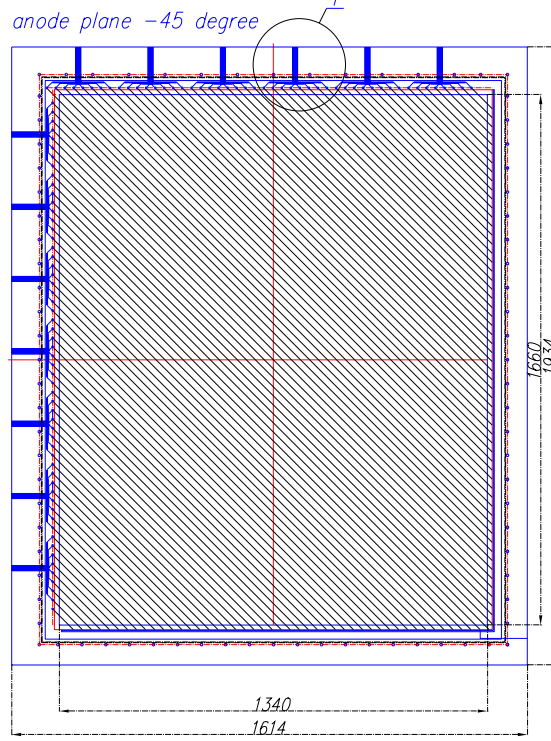


Figure 11: Dimensions and sense wire arrangement in one of the wire planes; all 12 planes are identical but for wire orientation; they are distributed into 4 chambers of 3 planes each.

The drift chambers and analyzer of the FPP will be mounted inside a sturdy frame, to facilitate its installation and removal; the frame and analyzers will be built by the University of Regina group (E. Brash et al: see part 6). Once the polarimeter is installed in the HMS focal plane, it will remain a part of its instrumentation, and will be interchangeable with the gas Čerenkov.

The crucial feature of the polarimeter is its figure of merit (FOM), defined as

FOM= $\int_{\vartheta_{min}}^{\vartheta_{max}} \epsilon(\vartheta) A_y^2(\vartheta) \sim \overline{\epsilon} \overline{A_y}^2$ , where  $\epsilon(\vartheta)$  is the differential fraction of events scattered in the analyzer at polar angle  $\vartheta$ , and  $A_y(\vartheta)$  is the corresponding analyzing power. The analyzing power of pp scattering is larger than that of the pC (graphite), hence adding hydrogen to the analyzer increases its FOM. As seen in Fig. 12, the pC analyzing power from experiment 93-027 decreases rapidly with increasing proton momentum up to 2.6 GeV/c, the maximum proton momentum of experiment 93-027.

In Figs. 13 and 14 we show the analyzing power data from experiment 99-007 for CH<sub>2</sub> up to proton momentum of 3.8 GeV/c, versus polar angle, and versus the  $p_{perp}$  with  $p_{perp} = p \sin \vartheta \sim \sqrt{-t}$ , respectively. We can see from these figures that the maximum value of the analyzing power decreases very little between 2.9 and 3.8 GeV/c proton momentum. These data lend themselves to a fairly secure extrapolation to higher energies as the  $p_{perp}$ -representation shows that the data approximately scales with  $p_{perp}$ .

Currently, the proton momenta for which we have complete angular distributions of the graphite analyzing power are  $\leq 2.6$  GeV/c from experiment 93-027 and  $\leq 3.2$  GeV/c from Saclay [46]; for pCH<sub>2</sub> it is 3.8 GeV/c from experiment 99-007 and for pp scattering it is 10 GeV/c [47].

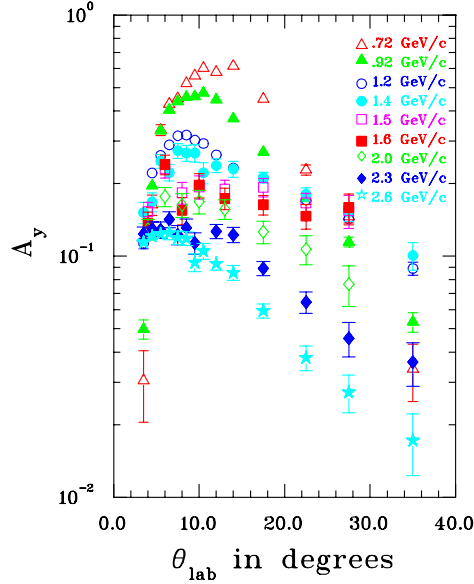


Figure 12: Results of of experiment 93-027 for the analyzing power of graphite, between 0.719 and 2.57 GeV/c proton momentum.

A calibration in the proton momentum range 3.8 to 5.5 GeV/c would be

helpful. Currently, the calibration is possible only at the Dubna Synchrotron. A proposal to do this calibration in June 2001 has been approved [48].

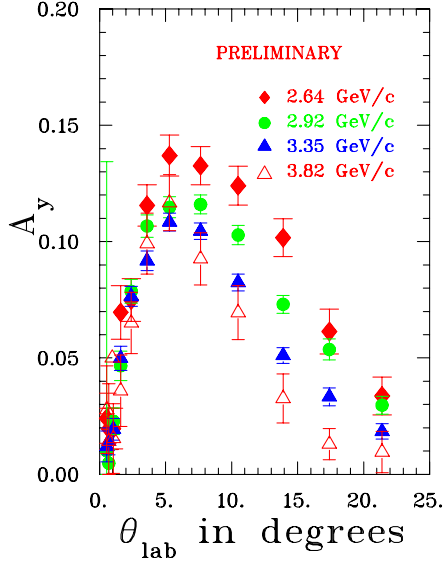


Figure 13: The analyzing power of  $\text{CH}_2$ ,  $A_y$ , between 2.64 and 3.81 GeV/c, versus  $\theta$ , from experiment 99-007.

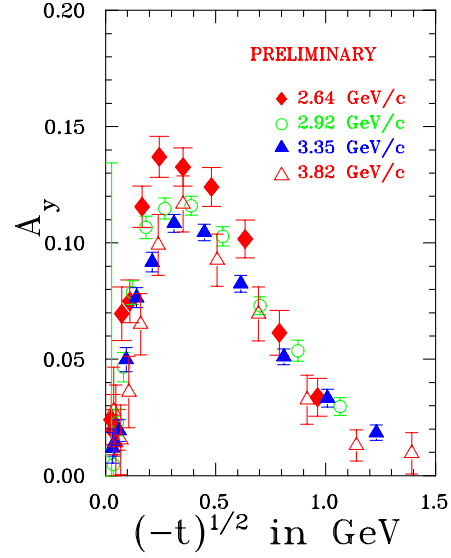


Figure 14: The same analyzing power of  $\text{CH}_2$ ,  $A_y$ , between 1.8 and 3.0 GeV versus  $\sqrt{-t} = p_{\text{perp}}$ , for the proton momenta of 99-007.

Again, addressing point 2 of the PAC 18 report on proposal 00-111, the design of this new FPP in Hall C is appropriate up to 10 GeV/c proton momentum (9.1 GeV kinetic energy), and therefore  $Q^2=17 \text{ GeV}^2$ ; this is defined by the material of the analyzer, the size of the chambers and analyzer, and the drift chamber resolution. Beyond this energy, the analyzing power of any material is likely to be too small for this technique. Large negative analyzing powers may become usable again at higher energies; however, the maximum momentum in the HMS is 7.5 GeV/c, limiting  $Q^2$  to  $12.4 \text{ GeV}^2$ .

#### 4.1.3 The Calorimeter

In order to fully separate the elastic ep events from all background events, we must detect the electron. Essential to this experiment is “solid angle matching”, which means that for each kinematics the solid angle of the electron detector must match the fixed solid angle of the proton detector, which is the HMS. With the beam energy fixed at 6 GeV, all the kinematics of this proposal have an electron scattering angle larger than the proton recoil angle; therefore the Jacobian for the electron is larger than that of the proton, and hence the solid

angle for the electron detector must be larger than that of the proton detector. Based on the design and tests for the Real Compton Scattering experiment in Hall A [14], and our recent use of this technique in experiment 99-007 in Hall A (see below), we can design a new calorimeter for Hall C with an angular resolution comparable to that of the HMS. The idea is to separate elastic ep scattering by selecting events with angles satisfying the 2-body kinematics; the better the angular resolution, the better the separation. Time information from each lead-glass block obtained with a TDC on each PM will be used to eliminate most of the accidental events. Our studies in Hall A, to be described below, indicate that the contribution of the target walls is negligible. The great advantage of Čerenkov lead-glass detectors is their relative insensitivity to pions and low energy particles.

Prior to experiment 99-007, in a test in May 2000, we re-measured the  $G_{Ep}/G_{Mp}$  ratio of experiment 93-027 at  $Q^2=3.0 \text{ GeV}^2$  by detecting the electron in an array of 45 lead glass blocks; the result was  $\mu_p G_{Ep}/G_{Mp} = 0.62 \pm 0.048$ , to be compared with the published results  $0.61 \pm 0.032$ ; the uncertainties given are statistical only.

The 3 new kinematics of experiment 99-007 used a larger calorimeter ( $3.3 \text{ m}^2$  frontal area) assembled from 147 lead glass blocks borrowed from the shower and pion-rejector detectors in Hall A. Signals from each PM were sent to TDCs and ADCs. The subsequent analysis indicated that the most important information was from the TDCs: a loose time cut eliminated most of the accidentals. The second most useful cut is on the vertical and horizontal angle correlation between electron and proton. Finally a relatively loose cut was applied on the missing energy calculated from the lead glass pulse height. This is best illustrated in Fig. 4.1.3, which at the top shows the difference between the proton momentum calculated from the proton angle and the measured proton momentum, without using any information from the calorimeter, and at the bottom with the 3 cuts just listed. The residual background under the two-body peak is of order 1%. During experiment 99-007, we took data at  $Q^2=3.5 \text{ GeV}^2$  again, but with 60 cm  $\text{CH}_2$  in the FPP, to compare with the 93-027 data obtained with 50 cm of C. This was also a check of consistency after exchange of the detector packages of the two HRS, which was necessitated by the need to detect protons with more than 3.2 GeV/c (in the left HRS). The electron was detected in the right HRS. No obvious difference in the optics was found, which would have resulted in a different spin transfer matrix. The new result,  $\mu_p G_{Ep}/G_{Mp} = 0.588 \pm 0.075$  is compatible with the published value  $\mu_p G_{Ep}/G_{Mp} = 0.609 \pm 0.047$ . This data point and the one at  $Q^2=3.0 \text{ GeV}^2$  mentioned above are included in the “preliminary” data shown in the various figures of the proposal.

The largest solid angle required in this experiment is 135 msr, at  $Q^2$  of 9  $\text{GeV}^2$ ; for this  $Q^2$  the new calorimeter will be located at  $68^\circ$ . To obtain the desired solid angle a calorimeter with a frontal area of  $2.5 \text{ m}^2$  will be located at a distance of 4.35 m from the target. We are planning to build this calorimeter with 1660  $3.9 \times 3.9 \text{ cm}^2$  lead-glass blocks, each read out by one ADC and one

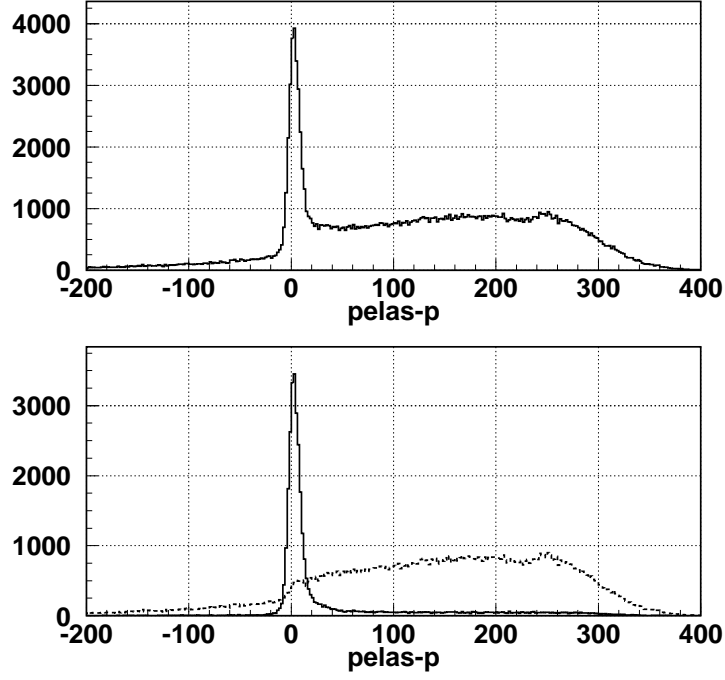


Figure 15: Single proton spectrum in the HRS for  $Q^2=5.6 \text{ GeV}^2$ , shown as the difference between calculated  $p(\theta)-p(\delta)$ . The two-body peak of elastic  $ep$  is at 0. The upper figure shows all events. The lower figure shows the same HRS spectrum with cuts on the electron timing, angular correlation and energy applied; also shown is the spectrum of the events removed by the cuts (dotted).

TDC. The expected position resolution is 3-5 mm, which will translate into an angular resolution of 1-2 mr when at the shortest distance to the target, to be compared with 17 mr for the Hall A calorimeter. Most of the accidentals will be eliminated by applying cuts on the TDC from each lead-glass block.

The primary responsibility for the calorimeter of this experiment will be with B. Wojtsekhowski (JLab, Hall A), H. Voskanyan (Yerevan/JLab Hall A) and V.P. Kubarovsky (Protvino).

## 5 The proposed measurements

In proposal 00-111 [10] submitted to JLab PAC18, we had proposed to measure the  $G_{Ep}/G_{Mp}$ -ratio for 3 new values of  $Q^2$ : 6.5, 7.5 and 9 GeV<sup>2</sup>, and a control point at 4.2 GeV<sup>2</sup> which coincides with one of 99-007. The PAC18 deferred its decision at the time, however the PAC expressed its conviction that the experiment was of great interest, and that the method was effective and precise.

Taking into account the analyzing power results of experiment 99-007, which are a bit smaller than the ones assumed in the proposal to PAC18, **we are now proposing 2 new data points: 7.5 and 9.0 GeV<sup>2</sup>, and as a control point, 4.2 GeV<sup>2</sup>**, the kinematics of these three points are in Table 1. The statistical uncertainties we propose to achieve are shown in Table 5 and illustrated in Fig. 5. The beam on target time required to achieve the error bars in Fig. 5 is 40 days.

The choice of  $Q^2=9$  GeV<sup>2</sup> is explained in Fig. 5 where the evolution of the statistical uncertainty versus the beam energy for a given  $Q^2$  is shown for a range of  $Q^2$ -values and equal duration, beam current and polarization, and with the calorimeter located so that its solid angle matches the HMS solid angle in all cases. Whereas the very best electron beam energy for  $Q^2=9$  GeV<sup>2</sup> is 7.5 GeV, the uncertainty is only 20% larger at an electron energy of 6 GeV, all other conditions being equal; we consider this a responsible and aggressive choice.

The viability of the technique has been fully verified in Hall A in tests and in experiment 99-007 in November-December 2000, as explained in section 4.1.3. All the CEBAF accelerator conditions required for this experiment are already achieved except the energy of 6 GeV: they call for a beam helicity of  $h=0.8$  and a current of 75  $\mu A$  incident on the standard 15 cm long LH<sub>2</sub> cell (unpolarized hydrogen). An energy of 6 GeV is an official target of CEBAF.

The HMS solid angle of 6 msr will be kinematically matched by the electron arm detector according to the reaction Jacobian for the electron, as explained in section 4.3.1. The calorimeter, with an active area of 2.5 m<sup>2</sup>, will be located at various distances from the target to maintain kinematical matching.

The anticipated uncertainties shown in Table 2 and in Fig.5 for the 4 data points (4.2, 7.5 and 9 GeV<sup>2</sup>) are evaluated from:

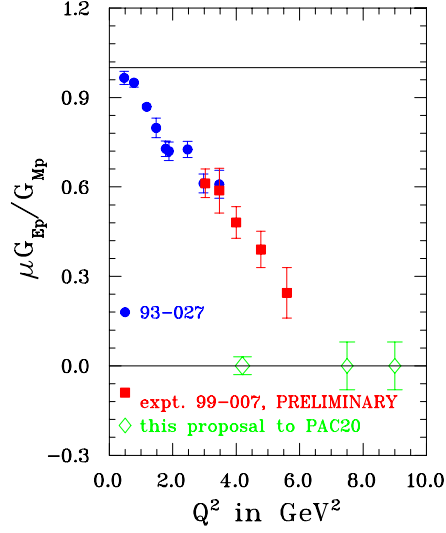


Figure 16: The  $\mu_p G_{Ep}/G_{Mp}$  results of experiments 93-027, 99-007 (PRELIMINARY) and proposed 00-111.

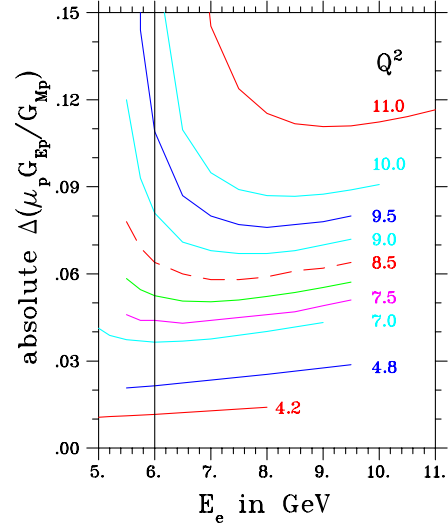


Figure 17: Evolution of the absolute statistical uncertainty on  $\mu_p G_{Ep}/G_{Mp}$  for various  $Q^2$ , versus beam energy.

$Q^2$ GeV <sup>2</sup>	$E_e$ GeV	$\theta_e$ deg	$E_{e'}$ GeV	$\theta_p$ deg	$p_p$ GeV/c	$d\sigma/d\Omega_e$ cm <sup>2</sup> /sr	$\epsilon A_y^2$ FOM	$\chi$ deg	$\Delta\Omega_e$ msr	rate Hz
4.2	4.0	46	1.7	24	3.0	$1.7 \times 10^{-34}$	$3.2 \times 10^{-3}$	152	22	105
7.5	6.0	46	2.0	17	4.8	$1.1 \times 10^{-36}$	$1.8 \times 10^{-3}$	236	37	12
9	6.0	68	1.2	11.4	5.66	$1.4 \times 10^{-37}$	$1.8 \times 10^{-3}$	274	135	6

Table 1: The 3 kinematics of this proposal. Note that the energy for  $Q^2=4.2$  GeV<sup>2</sup> is chosen such that  $\theta_e$  is the same as for  $Q^2=7.5$  GeV<sup>2</sup>



$Q^2$	$E_e$	absolute $\Delta(G_{Ep}/G_{Mp})$	time
GeV <sup>2</sup>	GeV		hours
4.2	4.8	0.04	40
7.5	6.0	0.08	200
9	6.0	0.08	720
		TOTAL TIME	960 or 40 days

Table 2: Absolute uncertainties, and times required.  $\Delta(\mu G_{Ep}/G_{Mp})$  is the anticipated absolute uncertainty. Here we assume that  $\mu G_{Ep}/G_{Mp}$  follows the fit to the existing JLab data, but the absolute uncertainty is essentially independent of  $\mu G_{Ep}/G_{Mp}$ .

$$\frac{\Delta(G_{Ep}/G_{Mp})}{G_{Ep}/G_{Mp}} = \sqrt{(\Delta a/a)^2 + (\Delta b/b)^2 + (\Delta \sin \chi / \sin \chi)^2} \quad (14)$$

where, for a given bin in  $\vartheta$ ,

$$\Delta a(\vartheta) = \Delta b(\vartheta) = \sqrt{\frac{2}{N_p^{fpp}(\vartheta)}} \quad (15)$$

where  $a$  and  $b$  are the amplitudes in Eq. 11 and 12, and  $N_p^{fpp}(\vartheta)$  is the number of protons scattered in  $\Delta\vartheta$  bin at polar angle  $\vartheta$  in the FPP. The main contribution to the absolute systematic uncertainty comes from  $\phi$ , the horizontal bending angle, rather than  $\theta$ , the vertical bending angle, as in the 2 previous experiments; it can be kept  $\leq 0.04$ .

This experiment will require time to measure the background in Hall C, to install the calorimeter and test it, to check the optical alignment of the HMS, to install the FPP in the HMS shield hut and test it. Table 5 shows an outline of the approximate times required.

## 6 Technical Considerations

In this part we review the technical changes or additions to the standard Hall C equipment which are required for this experiment, and estimate the cost to JLab or other sources.

what	goal	duration	conditions
lead-glass	background	1 day	parasitic
HMS optics	spin transport	1 day	dedicated
calorimeter	install	6 weeks	no beam
calorimeter	test	2 days	dedicated
polarimeter	install	1 month	no beam
polarimeter	test	2 days	dedicated
Total			80 days

Table 3: Approximate times for pre-testing, assembling and final testing of components in Hall C. Preliminary estimate of preparation time.

## Polarimeter

**FPP Chambers:** 4 drift chambers are required; a design based on the HADES/GSI chambers has been proposed by the Instrumentation group at JINR; the JINR group is a participant. A proposal to DOE has been prepared and will be sent as soon as this proposal is approved. Co-PI's are Perdrisat, Punjabi, Jones, Gilman and Piskunov. The amount requested (including students, travel and WM overhead) is \$254,824.-. This includes the on-chamber read-out boards, the low voltage power supplies, and a 5th chamber as a spare. E. Tomasi-Gustafsson will coordinate the chamber construction and has pledged up to \$50,000.- from DAPNIA/Saclay for supplies and electronics.

**TDC:** require 1248 channels of TDCs (LeCroy 1877); these can be borrowed from the Hall A FPP, including the FASTBUS crate and ROC; a dedicated read-out electronics package would be preferable.

**cabling:** the HV supplies and TDCs will be in the shielded hut (HMS); only short cables are required; the data stream will be brought upstairs with an additional ROC.

**Frame and analyzer:** building and installation will be the responsibility of the University of Regina group.

## Calorimeter

**Lead glass:** Approximately 1660 blocks are required. 700 blocks will come from the Hall A Real Compton Scattering experiment, under the responsibility of B. Wojtsekhowski and H. Voskanian. This will include the ADCs and HV power supplies, but not the TDCs. We will need an additional 700 ch. of TDCs for this: one solution is to use prototypes of the Hall D pipeline TDCs based on

the F1-chip; S. Wood will supervise the possible application of this project for our use; another is to use borrowed TDCs already at JLab.

Another 1000 lead glass blocks are coming from the IHEP in Protvino (responsible V.P. Kubarovsky) and are currently being moved from Fermilab where they have been used in experiment E871.

Box to contain detector and platform to elevate it to required height; to be built and paid for by JLab; estimated combined cost: 15 k\$ and 30 k\$, respectively. The platform built for RCS calorimeter can be used for this experiment.

**Electronics:** 1000 ch. of TDCs and 1000 channels of ADCs are being borrowed from Fermilab. This equipment will be moved to JLab as soon as this proposal is approved.

**discriminators:** for the TDCs; they may become available in Hall C.

**splitter:** to feed ADCs and discriminators for TDCs from each channel: 50 k\$ (JLab).

**additional patch panels:** for routing of calorimeter signals: 60 k\$ (JLab).

**cabling:** we are in the process of requesting 1000 signal+HV cables from Fermilab.

**power supplies:** we will need 1000 HV ch. and are in the process of arranging to borrow them from Fermilab. In addition three 200V DC supplies to boost the Protvino bases will be required; they need to have insulated grounds; cost 5 K\$ (JLab).

The Rutgers group (R. Gilman) will coordinate the calorimeter construction project and, in particular, will participate in designing and assembling the readout electronics.

### **Construction and installation of the two new detectors:**

The collaboration will design, build, install, test and commission the polarimeter and calorimeter. The collaboration will need JLab to provide for the qualified technical help and basic necessities (for example, gas for chambers, additional power lines). Appropriate laboratory space will be needed to assemble both detectors outside of Hall C, at JLab.

## 7 Conclusions

We propose to measure  $G_{Ep}/G_{Mp}$  to  $9 \text{ GeV}^2$  in an experiment in Hall C, detecting the proton in the HMS and the electron in a large solid angle lead glass calorimeter. Such an experiment is possible before the anticipated energy upgrade shut down. The interest of continuing this experiment is obvious from the recently published results of experiment 93-027 and the preliminary results of experiment 99-007, which we have shown here: the initially unexpected decrease of the ratio  $\mu_p G_{Ep}/G_{Mp}$  continues unabated to  $5.6 \text{ GeV}^2$ , indicating that the charge and magnetic distributions in the proton are markedly different at short distances.

Previous form factor data have been interpreted in terms of an early onset of the perturbative QCD limit:  $Q^2 F_2/F_1 \sim \text{constant}$ , as illustrated in Fig. 7. The new data from 93-027 and 99-007 clearly demonstrate that this is not the case at such a low  $Q^2$ . The  $Q^2$  region we will explore, when the proposed experiment is run, is potentially even more interesting: we could see a behavior similar to the one displayed by  $Q^4 G_{Mp}$  or  $Q^4 F_{1p}$ , around  $9 \text{ GeV}^2$ , or no such “asymptotic” behavior. In either case, characterizing  $F_{2p}$  to large  $Q^2$  will shed light on the spin dependence of the quark-quark interaction at short distances. More generally, accurate measurements of hadronic form factors serve as a crucial test which theories must pass before they can be applied to other reactions such as meson photo- and electro-production, real Compton scattering, or deuteron photo-disintegration. Finally, the observation that  $Q F_2/F_1$  becomes constant above  $\sim 2 \text{ GeV}^2$  is tantalizing; however, this fact cannot be interpreted as a failure of the perturbative QCD prediction until and unless new data at  $Q^2$  larger than  $5.6 \text{ GeV}^2$  become available.

The proposed measurement of  $G_{Ep}/G_{Mp}$  with small uncertainty and the existing cross section data [2, 15] together, will bring the experimental characterization of  $G_{Ep}$  and  $G_{Mp}$  to equal levels of accuracy in this important regime. Likewise, the combination of the proposed data with the existing cross section data, will determine both  $F_{1p}$  and  $F_{2p}$  with small uncertainty. Therefore, this experiment will extend the knowledge of  $F_{2p}$  to a  $Q^2$  region where, in the pQCD picture, spin flip should become strongly suppressed, or equivalently, helicity conservation should operate. A continuation of these measurements to  $9 \text{ GeV}^2$  is clearly of great interest. This  $Q^2$  region is often believed to be the one of transition between soft and hard scattering, the most challenging theoretically; but there are solidly motivated arguments that the behavior of  $Q^4 G_M$  or  $Q^2 F_2/F_1$  are not a signature of pQCD, but rather a consequence of the dominant role of soft processes in this  $Q^2$ -region. Ultimately, understanding of this difficult region will be achieved from QCD, the theory of strong interaction, and the data from this experiment will play an essential role toward this goal.

## References

- [1] M.K. Jones *et al.*, Phys. Rev. Lett. **84**, 1398 (2000).
- [2] L. Andivahis *et al.*, Phys. Rev. D **50**, 5491 (1994).
- [3] J. Litt *et al.*, Phys. Lett. B **31**, 40 (1970).
- [4] Ch. Berger *et al.*, Phys. Lett. B **35**, 87 (1971).
- [5] L.E. Price *et al.*, Phys. Rev. D **4**, 45 (1971).
- [6] W. Bartel *et al.*, Nucl. Phys. B **58**, 429 (1973).
- [7] B. Milbrath *et al.*, Phys. Rev. Lett. **80**, 452 (1998); erratum, Phys. Rev. Lett. **82**, 2221 (1999).
- [8] P. E. Bosted, Phys. Rev. C **51**, 409 (1995).
- [9] E. Brash and A. Kozlov, private communication.
- [10] JLab deferred experiment 00-111, C.F. Perdrisat, V. Punjabi, M.K. Jones and E. Brash.
- [11] <http://www.jlab.org/Hall-C/>
- [12] K. Wijesooriya *et al.*, accepted by Phys. Rev. Lett.(2001)
- [13] R. Gilman *et al.*, CEBAF proposal 94-012.
- [14] B. Wojtsekhowski *et al.*, CEBAF proposal 99-114.
- [15] R. G. Arnold *et al.*, Phys. Rev. Lett. **57**, 174 (1986); and A.F. Sill *et al.*, Phys. Rev. D **48**, 29 (1993). .
- [16] W.K. Brooks *et al.*, CEBAF proposal 94-017.
- [17] D.Day *et al.*, CEBAF proposal 93-026.
- [18] R. Madey *et al.*, CEBAF proposal 93-038.
- [19] S.J. Brodsky and G. Farrar, Phys. Rev. D **11**, 1309 (1975).
- [20] G. Höhler *et al.*, Nucl. Phys. B **114**, 505 (1976).
- [21] M.F. Gari and W. Kruempelmann, Z. Phys. A **322**, 689 (1985); M.F. Gari and W. Kruempelmann, Phys. Lett. B **247**, 159 (1992).
- [22] P. Mergell, U.G. Meissner, D. Drechsler Nucl. Phys. B **A596**, 367 (1996) ; and A.W. Hammer, U.G. Meissner and D. Drechsel, Phys. Lett. B **385**, 343 (1996).

- [23] P.L. Chung and F. Coester, Phys. Rev. D **44**, 229 (1991).
- [24] I. G. Aznauryan, Phys. Lett. B **316**, 391 (1993).
- [25] M.R. Frank, B.K. Jennings and G.A. Miller, Phys. Rev. C **54**, 920 (1996).
- [26] P. Kroll, M. Schurmann and W. Schweiger, Z. Phys. A - Hadrons and Nuclei **338**, 339 (1991).
- [27] A.V. Radyushkin, Acta Phys. Polnica B **15**, 40 (1984).
- [28] D.H. Lu, A.W. Thomas and A.G. Williams, Phys. Rev. C **57**, 2628 (1998).
- [29] G. Holzwarth, Zeitschr. Fuer Physik A **356**, 339(1996)
- [30] E. Pace, G. Salme, F. Cardarelli and S. Simula, Nucl. Phys. A **666&667**, 33c (2000).
- [31] M. De Sanctis, M.M. Giannini, L. Repeto and E. Santopinto, Phys. Rev. C **62**, 25208 (2000).
- [32] F. Cardarelli and S. Simula Phys. Rev. C **62**, 65201 (2000).
- [33] S.J. Brodsky and G.P. Lepage, Phys. Rev. D **22**, 2157 (1981).
- [34] J. Ralston, P. Jain and R. Buney, Proceedings of the Conf. on Intersections of Particle and Nuclear Physics, Québec City, (2000), ed. Z. Parseh and M. Marciano, AIP Conf. Proc. No. 549 (AIP, New York, 2000), p. 302.
- [35] X. Ji, Phys. Rev. D **55**, 7114 (1997), Phys. Rev. Lett. **78**, 610 (1997).
- [36] A.V. Radyushkin JLab-THY-98-10 and hep-ph/9803316 v2.
- [37] A.V. Afanasev hep-ph/9808291 v2.
- [38] A.V. Afanasev, private communication, 1999 and contribution to the “Exclusive and Semi-exclusive Processes at High Momentum Transfer, JLab 5/99.
- [39] J. Ashman *et al.*, Phys. Lett. B **206**, 364 (1988); D. Adams *et al.*, Phys. Rev. D **56**, 5330 (1997); and K. Abe *et al.*, Phys. Rev. D **58**, 112003 (1998)
- [40] N. Mathur, S.J. Dong, K.F. Liu, L. Mankiewicz and N.C. Mukhopadhyay, hep-ph/9912289
- [41] “Nuclear Theory with Lattice QCD”, a proposal to DOE, N. Isgur and J.W. Negele, PI’s (March 2000)
- [42] A.I. Akhiezer and M.P. Rekalo, Sov. J. Part. Nucl. **3**, 277 (1974).
- [43] R. Arnold, C. Carlson and F. Gross, Phys. Rev. C **23**, 363 (1981).

- [44] A.V. Afanasev, I. Akureshevich and N.P. Merenkov, hep-ph/0009273
- [45] <http://www.jlab.org/Hall-C/equipment/HMS/performance.html>
- [46] E. Chung *et al.*, Nucl. Inst. and Meth. in Phys. Res., A **363**, 561 (1994).
- [47] D. Miller *et al.*, Phys. Rev. D **16**, 2016 (1977); and Diebold *et al.*, Phys. Rev. Lett. **35**, 632 (1975); both data cover the energy of this proposal.
- [48] Proposal to JINR/Dubna PAC: "Measurement of analyzing powers for the reaction  $p + CH_2$  at polarized proton momentum 3-6 GeV/c", E. Tomasi-Gustafsson, N.M. Piskunov and C.F. Perdrisat, PT's, and 25 participants. Approved March 2001